Propofol induces metabolic reprogramming and cell death in a mitochondrial electron transport chain-dependent manner

Chisato Sumi[1,2], Akihisa Okamoto[2], Hiromasa Tanaka[2], Kenichiro Nishi[2], Munenori Kusunoki[1,2], Tomohiro Shoji[1,2], Takeo Uba[1,2], Yoshiyuki Matsuo[2], Takehiko Adachi[3], Jun-Ichi Hayashi[4], Keizo Takenaga[5] and Kiichi Hirota[2]

[1] Department of Anesthesiology, Kansai Medical University, Hirakata, Japan, [2] Department of Human Stress Response Science, Institute of Biomedical Science, Kansai Medical University, Hirakata, Japan, [3] Department of Anesthesiology, Tazuke Kofukai Medical Institute Kitano Hospital, Osaka, Japan, [4] University of Tsukuba, Tsukuba, Japan, [5] Department of Life Science, Shimane University Faculty of Medicine, Izumo, Japan

Correspondence:

Kiichi Hirota, MD, PhD

Department of Human Stress Response Science

Institute of Biomedical Science

Kansai Medical University

2-5-1 Shin-Machi, Hirakata, Osaka 573-1010, Japan

Tel: +81-72-804-2682

e-mail: hif1@mac.com

Abstract

The intravenous anesthetic propofol (2,6-diisopropylphenol) has been used for the induction and maintenance of anesthesia in operating rooms and for sedation in intensive care units. Although there is no widely accepted definition of propofol infusion syndrome (PRIS), PRIS is defined as the development of metabolic acidosis, rhabdomyolysis, hyperkalemia, hepatomegaly, renal failure, arrhythmia, and progressive cardiac failure. In vitro evidence suggests that PRIS is related to the impaired mitochondrial function. There are indications that preexisting mitochondrial disorders predispose to PRIS. However, the precise molecular mechanisms, including mitochondrial defects and metabolic reprogramming of PRIS, are largely unknown as yet. To elucidate the underlying cellular and molecular mechanisms of PRIS, we investigated the effects of propofol on the cellular metabolic mode and cell death. We demonstrated that clinically relevant concentrations of propofol used within a clinically relevant exposure time suppressed the mitochondrial function, induced generation of reactive oxygen species and induced the metabolic reprogramming, from oxidative phosphorylation to glycolysis, by targeting complexes I and III of mitochondria. The data also indicated that a predisposition to mitochondrial dysfunction, caused by a genetic mutation or pharmacological suppression of the electron transport chain by biguanides such as metformin and phenformin, promoted the cell death and caspase activation induced by propofol.

Introduction

Since its introduction into clinical practice in 1986, propofol (2,6-diisopropylphenol) has been used for the induction and maintenance of anesthesia in operating rooms and for sedation in intensive care units [1]. Although propofol is considered a safe agent for anesthesia and sedation, a rare but severe complication can occur, especially in patients receiving high doses of the anesthetic for prolonged periods. A number of clinical reports have indicated a serious side effect of propofol, propofol infusion syndrome (PRIS) [2]. Since PRIS was first described in 1992 [3], the clinical awareness and research interest into this disorder have continued to grow. The medical literature now includes over 100 published case reports, case series, letters, reviews, and random experiments. Nonetheless, the exact incidence and etiology of PRIS remain unclear at present. Although there is no widely accepted definition of PRIS, PRIS is defined as the development of metabolic acidosis (lactic acidosis), rhabdomyolysis, hyperkalemia, hepatomegaly, renal failure, arrhythmia, and progressive cardiac failure [2]. There is a strong association between PRIS and propofol infusion at doses greater than 4 mg/kg/h and an exposure longer than 48 h, although the precise molecular mechanisms of PRIS have not been elucidated. In vitro evidence suggests that PRIS is related to impaired mitochondrial function [4]. There are indications that preexisting mitochondrial disorders predispose to PRIS [4-6]. Moreover, studies using isolated mitochondria have demonstrated that propofol showed an effect on the mitochondrial respiratory chain. A decrease in the transmembrane electrical potential ($\Delta\Psi$) has been reported in liver mitochondria isolated from rats incubated with propofol [7]. An increase of the oxygen consumption rate (OCR) has suggested that propofol acts as an uncoupler in oxidative phosphorylation (OXPHOS) [8]. It has also been indicated that incubation of isolated mitochondria from rats with high concentrations of propofol (100 to 400 μM) resulted in a strong inhibition of the activity of complex I and, to a lesser degree, of complexes II and III [9]. Other reports have also demonstrated a reduction of complex IV activity in skeletal muscles,

which led to a hypothesis that a propofol metabolite causes a disruption of the respiratory chain [10].

However, the precise molecular mechanisms, including the relationship between mitochondrial defects and metabolic reprogramming in the pathophysiology of PRIS, are largely unknown as yet. To investigate the underlying cellular and molecular mechanisms of PRIS, we investigated the effects of propofol on cell life and death, oxygen metabolism, and mitochondrial function using cells of various origins, in particular, transmitochondrial cybrid cells harboring a mitochondrial DNA defect and mutations. We demonstrated that clinically relevant concentrations of propofol used within a clinically relevant exposure time suppressed the mitochondrial function, induced generation of reactive oxygen species (ROS) and induced the metabolic reprogramming [11], from OXPHOS to glycolysis, by targeting complexes I and III of mitochondria. The data also indicated that a predisposition to mitochondrial dysfunction, caused by a genetic mutation or pharmacological suppression of the electron transport chain (ETC) in mitochondria by biguanides such as metformin and phenformin, promoted the cell death and caspase activation induced by propofol.

Results

Propofol induced activation of caspases and cell death in a concentration- and time-dependent manner

To determine whether propofol activates signaling pathways of cell death, we examined the concentration- and time-response relationship between propofol and caspase-3/7 activation. Neuronal SH-SY5Y cells were treated with the indicated concentrations of propofol (Fig. 1a) and for the indicated times (Fig. 1b). Concentrations of propofol higher than 50 μM induced caspase activation within 6 h (Fig. 1a), and 50 μM propofol induced the activation in a time-dependent manner up to 12 h (Fig. 1b). Importantly, 25 μM propofol, which did not induce caspase-3/7 activation within 6 h (Fig. 1a), induced the activation at 12 h (Fig. 1b). Next, the activity of caspase-9 was evaluated. Similar to the activation of caspase-3/7, propofol at concentrations higher than 50 μM activated caspase-9 (Fig. 1c). In contrast, release of lactate dehydrogenase (LDH) only increased when cells were treated with propofol concentrations higher than 150 μM (Fig. 1d). To confirm the relationship between these findings and cell death, SH-SY5Y cells were stained with propidium iodide (PI) and recombinant fluorescein isothiocyanate (FITC)-conjugated annexin V, and the proportion of dead cells was evaluated by flow cytometry (Figs. 1e and 1f and Supplementary Fig. 1). Consistent with the activation of caspase-3/7 and caspase-9, treatment with different concentrations of propofol caused cell death in a concentration- (Fig. 1e) and time-dependent manner (Fig. 1f). Next, the mitochondrial membrane voltage ($\Delta\Psi m$) was investigated, and propofol at concentrations more than 50 μM decreased $\Delta\Psi m$ within 6 h (Fig. 1g). In addition, propofol at concentrations higher than 50 μM suppressed the cell viability, measured by an MTS assay (Supplementary Fig. 2a).

2,4-diisopropylphenol, commonly known as 2,4-propofol, is an isomeric form of propofol. We tested the effects of 2,4-diisopropylphenol on caspase-3/7 activation in SH-SY5Y cells. Similar to propofol, 2,4-diisopropylphenol induced caspase-3/7 activation within 6 h (Supplementary Fig. 2b). Interestingly, 25 μM 2,4-diisopropylphenol could activate caspase-3/7 within 6 h,

suggesting that 2,4-diisopropylphenol is a more toxic apoptosis inducer than propofol. Next, the effects of propofol were investigated in cells of different origins, including mouse myoblast C2C12 cells (Supplementary Fig. 2c), human cervical cancer HeLa cells (Supplementary Fig. 2d), and Lewis lung carcinoma P29 cells (Supplementary Fig. 2e). Similar to its effects on SH-SY5Y cells, 50 and 100 μM propofol but not 12.5 or 25 μM propofol induced caspase-3/7 activation in the other cell lines within 6 h.

Propofol suppressed oxygen metabolism and induced metabolic reprogramming

Next, we investigated the effects of propofol on oxygen metabolism and glycolysis in SH-SY5Y cells by assaying OCR and the extracellular acidification rate (ECAR), which is a surrogate index for glycolysis. SH-SY5Y cells were preincubated with the indicated concentrations of propofol for the indicated periods. The mitochondrial OCR was significantly suppressed by the treatment with 50 μM propofol for 6 h (Fig.s 2a and 2b, Supplementary Figs. 3a and 3c–f). Accordingly, the ECAR levels, representing the extracellular lactate concentration, were significantly higher upon the treatment with 50 μM propofol (Figs. 2c and 2d, Supplementary Figs. 3b). Propofol at a concentration of 25 μM, which exerted no significant effects within 6 h, suppressed OCR (Fig. 2e) and enhanced ECAR (Fig. 2f) after 12 h of incubation. Thus, the evidence indicates that propofol affects the oxygen metabolism in mitochondria. It has been reported that the disturbance of mitochondrial ETC leads to generation of reactive oxygen species (ROS) by cells [12,13]. ROS generation was observed in SH-5Y5 cells in response to propofol exposure within 3 h (Fig. 2g).

Involvement of mitochondria and ROS in propofol-induced caspase activation and cell death

As shown in figure 2, propofol affected the mitochondrial ETC and intracellular oxygen metabolism in SH-SY5Y cells. To examine the involvement of mitochondria in

propofol-induced cell death, we used the P29 cell line and its derivative ρ0P29, which lacks the mitochondrial DNA (mtDNA) [14, Ishikawa, 2008 #64, Ishikawa, 2008 #8]. P29 and ρ0P29 cells were exposed to the indicated concentrations of propofol for 6 h, and then the activity of caspase-3/7 (Fig. 3a) and cell death (Fig. 3b) were assayed. Both caspase-3/7 and cell death assays indicated that, unlike P29 cells, ρ0P29 cells were completely resistant to 50 μM and partially to 100 μM propofol after 6 h of incubation (Figs 3a and 3b). Together with the results showing that propofol affects the ETC function of mitochondria, this evidence strongly suggests that mitochondria play a critical role and are a target in propofol-induced cell death.

Effects of propofol on the activity of ETC complexes

Next, we assayed the effects of propofol on the activity of mitochondrial respiratory chain complexes I–IV in live cells using the Extracellular Flux Analyzer™ (Figs. 4a–d). The results indicated that propofol significantly suppressed the activity of complexes I and III but not II or IV.

Mitochondrial ETC inhibitors synergistically enhanced propofol toxicity

Next, we investigated the effects of several ETC inhibitors on the propofol-induced caspase-3/7 activity in SH-SY5Y cells. Cells were exposed to rotenone (100 nM), antimycin A (25 μg/mL), or oligomycin (4 μM), with or without indicated concentrations of propofol, for 6 h, and caspase-3/7 activity was assayed. Neither 100 nM rotenone, 25 μg/mL antimycin, 4 μM oligomycin, nor 12.5 μM or 25 μM propofol alone induced caspase-3/7 activation within 6 h (Fig. 5a). On the other hand, 12.5 and 25 μM propofol activated caspase-3/7 in the presence of rotenone, antimycin A , and oligomycin (Figs. 5a). Similarly, 12.5 and 25 μM propofol with rotenone induced cell death within 6 h (Fig. 5b). This evidence indicates that cooperative inhibition of mitochondria by both propofol and the ETC inhibitors induces cell death at even clinically relevant concentrations of propofol within 6 h.

Genetic predisposition to mitochondrial dysfunction increased propofol-induced caspase activation and cell death

For further study, we adopted transmitochondrial cybrids carrying mtDNA with defined pathogenic mutations. mtDNA donors and ρ0P29 cells were used to obtain transmitochondrial cybrids P29mtA11, P29mtB82M, P29mtCOIM, and P29mtΔ (Tables 1 and 2) [15], and oxygen metabolism profiles of these clones were examined (Figs. 6a and 6b). These transmitochondrial cybrids were exposed to the indicated concentrations of propofol for 6 h to investigate the caspase-3/7 activation and cell death. Interestingly, in contrast to parental P29 cells, caspase-3/7 activation was induced in P29mtA11, P29mtB82M, and P29mtCOIM cells even with 12.5 μM propofol (Fig. 6c). In contrast, P29mtΔ cells, similar to ρ0P29 cells, were completely resistant to 50 μM propofol and partially resistant to 100 μM propofol (Fig. 6d). The cell death flow cytometry assay also indicated that 25 μM propofol induced the cell death within 6 h in P29mtA11, P29mtB82M and P29mtCOIM cells (Fig. 6d). Thus, our experimental results indicated that cells harboring genetic mutations in mtDNA (*ND6* in complex I or *COI* in complex IV) were more susceptible to propofol.

Pharmacological suppression of mitochondrial ETC increased propofol-induced caspase activation and cell death

The biguanides metformin and phenformin are widely used to reduce high blood sugar levels caused by diabetes [16]. Metformin and phenformin have also been shown to suppress complex I of ETC, which is used by cells to generate energy [17-21]. To confirm the effect of blockade of ETC, SH-SY5Y cells were pretreated with 2.5–20 mM metformin or 5–15 μM phenformin for 6 h, with or without indicated concentrations of propofol, and then the cells were tested using the OCR and ECAR assays. Incubation for 6 h with either 2.5 mM metformin or 5 μM phenformin did not affect OCR (Fig. 7a and Supplementary Fig. 4a) and ECAR (Fig. 7b and Supplementary

Fig. 4b) in SH-SY5Y cells. In contrast, not only 25 μM but also 12.5 μM propofol, which did not affect OCR or ECAR, significantly decreased OCR (Fig. 7a) and increased ECAR (Fig. 7b) in the presence of 2.5 mM metformin. Next, we investigated ROS generation upon cell exposure to 25 μM propofol with or without 5 mM metformin. Exposure to 25 μM propofol did not induce ROS generation without metformin. With metformin, however, 25 μM propofol induced ROS generation (Fig. 7c). Then, SH-SY5Y cells were tested for caspase 3/7 activation (Fig. 7d) and cell death (Fig. 7e) after treatment with 5 mM metformin or 5 μM phenformin (Supplementary Figs. 4c and 4d) for 6 h, with or without indicated concentrations of propofol. Metformin at 5 mM and phenformin at 5 μM increased the propofol-induced caspase-3/7 activation and cell death.

Discussion

In this study, we demonstrated for the first time that propofol at clinically relevant concentrations and within clinically relevant incubation times altered the oxygen metabolism by targeting mitochondrial complexes I and III and induced the cellular metabolic reprogramming, from OXPHOS to glycolysis. The suppression of mitochondria elicited the cell death in cell lines of various origins, including transmitochondrial cybrids carrying mtDNA with defined pathogenic mutations.

The concentrations of propofol tested in this study varied from 12.5 to 150 μM. It has been reported that the plasma concentrations of propofol during anesthesia and sedation are from 2 μg/mL (11 μM) up to 5 μg/mL (27.5 μM) [22]. The concentration of propofol was also measured in tissue samples from rats treated with propofol at a dose of 20 mg/kg/h, and the study indicated that the tissue concentration of propofol could reach 200 μM under certain conditions [23]. Thus, the evidence indicates that the concentrations of propofol adopted in this study were clinically relevant. The times of exposure used in this study ranged from 3 to 12 h, which was also within the clinically relevant duration of exposure.

Although predictive factors for PRIS have not been established, there is a consensus that exposure to high doses of propofol for prolonged periods is the most critical risk factor for PRIS [1,2,6,24]. In this study, we demonstrated that propofol at concentrations higher than 50 μM but not at or below 25 μM showed cell toxicity within 6 h (Figs. 1a–e). On the other hand, even 25 μM propofol significantly increased caspase activity and cell death during incubation for 12 h (Figs. 1b and 1f). We also simultaneously measured OCR and ECAR in live cells treated with propofol (Figs. 2a–2d). Propofol at 50 μM significantly suppressed OCR and increased ECAR. At 100 μM, propofol inhibited both OCR and ECAR (Figs. 2b and 2d, Supplementary Figs. 3g and 3h), which may be due to the cell death induced by 100 μM propofol. The evidence indicates that propofol suppresses OXPHOS in mitochondria and induces metabolic reprogramming, from OXPHOS to glycolysis, resulting in the generation of lactate. This

metabolic reprogramming is one of the most critical cellular mechanisms of lactic acidosis observed in PRIS [1]. PRIS is defined as the development of metabolic acidosis (lactic acidosis), rhabdomyolysis, and hyperkalemia [2]. The cell death and acceleration of glycolysis can be explained by the toxicity of and suppression of oxygen metabolism in mitochondria by propofol.

As clearly demonstrated in this and other studies [25-28], propofol induces cell death. Not only neuronal SH-SY5Y cells but also cells of other origins, such as C2C12 muscle cells, HeLa cervical carcinoma cells, and P29 lung cancer cells, are susceptible to propofol. There are at least two known modes of cell death, apoptosis and necrosis. Apoptosis is a strictly regulated or programmed process involving the activation of specific proteases, which are responsible for organized removal of damaged cells [29]. Apoptosis involves the regulated activity of catabolic enzymes (proteases and nucleases) within a near-to-intact plasma membrane and is commonly accompanied by characteristic changes in nuclear morphology and chromatin biochemistry. In this study, propofol treatment promoted the caspase-3/7 and caspase-9 activation. These data indicate that propofol activates the apoptosis pathway. Meanwhile, the flow cytometry analysis demonstrated that treatment of cells with propofol concentrations greater than 150 μM also resulted in LDHA release (Fig. 1d) and increased numbers of PI- and annexin V-positive cells (Fig. 1e and Supplementary Fig. 1). These data strongly suggest that propofol elicits both types of cell death depending on the concentration. Another important finding of this study is the relationship between the cell death and the duration of incubation with propofol. At 50 μM, propofol induced cell death within 6 h (Fig. 1f). On the other hand, 12.5 or 25 μM propofol did not induce caspase-3/7 activation or cell death within the same time (Fig. 1a). However, 25 μM propofol significantly induced caspase-3/7 activation after the incubation for 12 h (Fig. 1b). This cellular response to propofol represents one of the clinically important characteristics of PRIS.

As demonstrated in figures 2 and 3, propofol inhibited the mitochondrial ETC in a time- and concentration-dependent manner. In this study, we measured activity of each ETC complex in live cells using an extracellular flux analyzer. Importantly, the experimental results indicated that complexes I and III were the targets of propofol in the mitochondrial ETC (Figs. 4a and 4c). Several studies have been reported that used isolated mitochondria, and some have suggested that propofol inhibits complex II and complex IV activity. However, out study using live cells indicated that propofol does not affect the activity of complex II or complex IV. Another finding in this report was that propofol induced ROS generation (Fig. 2g). And while the precise origin of these ROS remains unclear, our findings strongly suggest that mitochondria play a critical role in this process. It is demonstrated thta disturbance of mitochondria leads to increased production of ROS by the ETC [12,13]. As such, these data imply that propofol-mediated cell death is dependent on mitochondria. Consistent with this conclusion, the mitochondrial DNA-deficient ρ0 cells were resistant to propofol treatment (Fig. 3).

Based on the results of a multicenter study of 1,017 critically ill patients from 11 academic medical centers, who were administered an infusion of propofol for more than 24 h, the incidence of PRIS slightly exceeds 1% [30]. Although no definitive predictive factors or markers are known for PRIS, there is a strong association between PRIS and propofol infusions at doses greater than 4 mg/mg/h and for longer than 48 h [2]. In addition, an association between PRIS and mitochondrial defects is considered to be critical. Mitochondrial disease, once thought to be a rare clinical entity, is now recognized as an important cause of a wide range of neurological, cardiac, muscle, and endocrine disorders [4,5]. The respiratory chain consists of five complexes, each containing multiple protein subunits. The number of subunits ranges from 4 for complex II to at least 46 for complex I. It is obvious that mutations in more than 100 genes can directly affect the function of the respiratory chain, and there are perhaps more than 1,000 genes that can indirectly affect the respiratory chain or other aspects of metabolism. It has been reported that

complex I is uniquely sensitive to many anesthetic agents [31]. To approach the issue, we adopted cells harboring mtDNA mutations [15,32,33]. As shown in figures 3 and 6, ρ0P29 cells are resistant to 50 μM propofol. P29mtΔ cells, carrying the nuclear genome of P29 cells and the mitochondrial genome of ΔmtDNA4696, with a 4,696-bp deletion [32], are also resistant to propofol (Figs. 6c and 6d). In contrast, P29mtA11 cells with the G13997A mutation in mtDNA and P29mtB82M cells with the 13885insC insertion, both of which affect the NADH-ubiquinone oxidoreductase chain 6 (ND6) protein of complex I, are more sensitive to propofol than P29 cells are. Propofol at 12.5 and 25 μM induced the caspase-3/7 activation and cell death in both mutant cell lines within 6 h (Fig. 6c). P29mtCOIM cells with a missense mutation in cytochrome c oxidase I (COI) are as sensitive to propofol as P29 cells. This evidence indicates that cells with mutations in mtDNA are more sensitive to propofol. Thus, the results are consistent with the consensus that not only does PRIS occur in mitochondrial disorder patients, but mitochondrial disorder patients are likely to be at higher risk of developing PRIS [4,34,35].

In addition to the genetic mutations affecting mitochondrial function, pharmacological disturbance of mitochondria with biguanides, including metformin and phenformin, also synergistically suppressed the mitochondrial function and induced caspase activation and cell death. The primary effect of biguanides is generally thought to be the inhibition of respiratory complex I (NADH:ubiquinone oxidoreductase), which leads to the energy stress by decreasing ATP synthesis by OXPHOS [17,18,36,37]. In addition, a number of studies have indicated that biguanides also affect complexes II, III, and IV and F1F0-ATPase [19,38]. Metformin and phenformin are used as antidiabetic drugs and are associated with lactic acidosis. We demonstrated that both metformin and phenformin increased ECAR (Fig. 7b and Supplementary Fig. 4b) and decreased OCR (Fig. 7a and Supplementary Fig. 4a), which indicates the metabolic reprogramming. A study has indicated that accumulation of positively charged molecules such as metformin and phenformin in the mitochondrial matrix in response to the generation of the

proton-motive force across the inner mitochondrial membrane is a well-described physical phenomenon. Because of this, intramitochondrial biguanide concentrations are raised far above their external concentrations, with approximately 100-fold accumulation observed in mitochondria of cultured cells compared to the concentration in the external medium [37]. Thus, it is possible that metformin accumulates in tissues of patients at levels of complex I inhibition. In this study, we adopted biguanides as mitochondrial inhibitors. Other clinically used drugs, including chloramphenicol [39,40] aspirin [41,42], statins [17], and local anesthetics [43], also inhibit mitochondrial functions. Our experimental results suggest that preexposure to mitochondrial inhibitors before propofol administration may increase the toxicity of propofol, resulting in PRIS.

In conclusion, clinically relevant concentrations of propofol used within a clinically relevant exposure time suppressed the mitochondrial function, and induced generation of ROS and induced the metabolic reprogramming, from OXPHOS to glycolysis, by targeting complexes I and III of mitochondria. Our data also indicated that a predisposition to mitochondrial dysfunction, caused by genetic mutations and pharmacological suppression of ETC by biguanides such as metformin and phenformin, promoted the cell death and caspase activation induced by propofol. The process is likely to constitute the molecular basis of PRIS (Fig. 8).

Materials and Methods

Reagents

Propofol (2,6-diisopropylphenol), 2,4-diisopropylphenol, dimethyl sulfoxide (DMSO) were obtained from Sigma-Aldrich (St. Louis, MO, USA). Rotenone, oligomycin and antimycin A are obtained from Abcam, Inc. (Cambridge, MA, USA).

Cell lines and cell culture

Established cell lines derived from the human neuroblastoma SH-SY5Y cells and cervical carcinoma (HeLa cells) were maintained in RPMI 1640 medium supplemented with 10% fetal bovine serum, 100 U/mL penicillin, and 0.1 mg/mL streptomycin. The mouse cell lines and their characteristics are listed in Tables 1 and 2. P29 cells originated from Lewis lung carcinoma (C57BL/6 mouse strain), and B82 cells are fibrosarcoma cells derived from the L929 fibroblast cell line (C3H/An mouse strain) [15,32,44]. Parental P29 cells, ρ0 cells, and the transmitochondrial cybrids were grown in Dulbecco's modified Eagle's medium supplemented with pyruvate (0.1 mg/mL), uridine (50 mg/mL), and 10% fetal bovine serum. We isolated ρ0 cells by treating parental P29 cells with 1.5 mg/mL ditercalinium, an antitumor *bis*-intercalating agent. Enucleated cells of mtDNA donors were prepared by pretreatment with cytochalasin B (10 μg/mL) for 2 min, followed by centrifugation at 7,500 × *g* for 10 min [15]. The resultant cytoplasts were fused with ρ0 cells using polyethylene glycol. The transmitochondrial cybrids (see Table 2) were isolated in a selection medium that allows exclusive growth of the cybrids [15].

Cell growth MTS assay

Cell growth was assessed using a CellTiter 96 AQueous One Solution Cell Proliferation Assay™ (Promega, Madison, WI, USA) [43,45]. Briefly, cells were seeded into 96-well plates (2 × 10^4 cells/well) and cultured overnight. On the following day, the cells were treated with the indicated concentrations of the appropriate drug(s) for varying times. After the treatment, 20 μL of the CellTiter 96 AQueous One Solution™ reagent was added to each well, the plates were incubated at 37 °C for 1 h, and the absorbance of each sample was measured using an iMark™ microplate reader (Bio-Rad, Hercules, CA, USA) at a wavelength of 490 nm. Cell viability was calculated by comparing the absorbance of treated cells with that of the control cells incubated without drugs, which was defined as 100%. All samples were tested in triplicate or quadruplicate in each experiment.

Caspase-3/7 and caspase-9 activity assays

Activity levels of caspase-3/7 and caspase-9 were assessed using an Apo-ONE™ Homogeneous Caspase-3/7 Assay Kit (Promega) and a Caspase-Glo™ 9 Assays Kit (Promega), respectively, according to the manufacturer's protocols [43,45]. Briefly, cells were seeded into 96-well plates (2 × 10^4 cells/well) and incubated overnight. On the following day, the cells were treated with the indicated concentrations of the appropriate drug(s) for varying times. After the treatment, 100 μL of Apo-ONE Caspase-3/7 Reagent™ was added to each well. The plates were incubated at room temperature for 1 h, and the luminescence of each well was measured using an EnSpire™ multimode plate reader (PerkinElmer, Waltham, MA, USA). Caspase activity was calculated by comparing the levels of luminescence of the treated cells with that of the control cell population incubated without drugs, which was defined as 100%. The assays were performed in triplicate at least twice. Data were expressed as the mean ± standard deviation (SD).

Analysis of cell death

The protocol was described previously [43,45]. Briefly, the levels of cell apoptosis were measured using an Annexin V–FITC Apoptosis Detection kit (BioVision, Milpitas, CA, USA), according to the manufacturer's instructions. For the analysis, cells were seeded into 6-well plates (3×10^5 cells/well) and incubated overnight. On the following day, the cells were treated with the indicated concentrations of the appropriate drug(s) for varying times and harvested by centrifugation at 1,200 rpm for 3 min. The cell pellets were resuspended in a mixture comprised of 500 μL of binding buffer, 5 μL of Annexing V–FITC, and 5 μL of PI (50 μg/mL). The suspensions were incubated for 5 min at room temperature in the dark and analyzed using a FACSCalibur flow cytometer (BD Biosciences, San Jose, CA, USA) equipped with the CellQuest Pro™ software. The data were evaluated using the FlowJo™ version 9.9.4 software (TreeStar, Ashland, OR, USA), then exported to Excel spreadsheets, and subsequently analyzed using the statistical application GraphPad™ Prism 7.

Determination of mitochondrial membrane potential

The mitochondrial membrane potential ($\Delta\Psi m$) was determined by flow cytometry using a MitoPT™ JC-1 assay kit (ImmunoChemistry Technologies, Bloomington, MN, USA), according to the manufacturer's instructions [45]. For the analysis, cells were seeded into 6-well plates (3×10^5 cells/well) and cultured overnight. On the following day, the cells were treated with the indicated concentrations of the appropriate drug(s) for varying times and then pelleted by centrifugation at 1,200 rpm for 3 min. The cells were then resuspended in JC-1, incubated at 37 °C for 15 min in the dark, and collected by centrifugation at 1,200 rpm for 3 min. The cell pellets were resuspended in 500 μL of assay buffer. The samples were subsequently analyzed using a FACSCalibur flow cytometer (BD Biosciences) equipped with the CellQuest Pro™ software for the detection of red JC-1 aggregates (590 nm emission) or green JC-1 monomers (527 nm emission). The data were evaluated using the FlowJo version 7.6.3 software (TreeStar),

then exported to Excel spreadsheets, and subsequently analyzed using the statistical application Prims7™.

Lactate dehydrogenase (LDH)-based cytotoxic assay

Cell cytotoxicity was measured using CytoTox-ONE™ Kit (Promega) as described previoulsy [43,45]. Briefly, cells were cultured overnight in 96-well plates (2×10^4 cells/well) and treated with the indicated drug(s) for varying lengths of time. Twenty µl of CytoTox-ONE™ reagent was added to each well and plates were incubated at 22 °C for 10 min. The reaction was terminated by adding 50 µl of Stop Solution, and the fluorescence was recorded with an excitation wavelength of 560 nm and an emission wavelength of 590 nm using an EnSpire™ Multimode Plate Reader (PerkinElmer). The percentage of cell death was determined by comparing the release of LDH (fluorescence value) from each treatment group with that of the positive control treated with Lysis solution, which was defined as 100 %. Meanwhile, the value for LDH release from untreated cells (negative control) was defined as 0 %. Each sample was assayed in triplicate.

Measurement of ROS Generation

ROS generation was detected with 2' ,7' -dichlorofluorescin diacetate (DCFH-DA) (Molecular Probes, Eugene, OR). Briefly, the cells cultured in 35-mm-diameter glass-bottom culture dishes (Mat- Teck, Ashland, MA) were incubated with 10 M DCFH-DA for 10 min at 37 °C in serum-free DMEM, washed twice with Dulbecco's phosphate-buffered saline (DPBS) or analyzed with a flow cytometer (Beckton Dickinson). Mean fluorescence intensity was analyzed using CellQuest software (Becton Dickinson).

Cellular oxygen consumption and extracellular acidification measurement

Cellular OCR and ECAR were determined with the XF Cell Mito Stress Test™ and XF Glycolysis Stress Test™, respectively, using an XFp Extracellular Flux Analyzer™ (Seahorse Bioscience, USA) [43]. Cells (2×10^5 cells/well) were seeded into an XFp cell culture microplate, and OCR was assessed in glucose-containing XF base medium according to the manufacturer's instructions. The sensor cartridge for the XFp analyzer was hydrated in a 37 °C non-CO_2 incubator on the day before the experiment. For the OCR assay, injection port A on the sensor cartridge was loaded with 1.5 μM oligomycin (complex V inhibitor), port B was loaded with 2 μM carbonyl cyanide-4-(trifluoromethoxy)phenylhydrazone (FCCP), and port C was loaded with 0.5 μM rotenone/antimycin A (inhibitors of complex I and complex III). During the sensor calibration, cells were incubated in a 37 °C non-CO_2 incubator in 180 μL of assay medium (XF base medium with 5.5 mM glucose, 1 mM pyruvate, and 2 mM L-glutamine, pH 7.4). The plate was immediately placed into the calibrated XFp extracellular flux analyzer for the Mito Stress test (Supplementary Fig. 3a). The assay parameters were calculated as follows: OCR (basal) = (last rate measurement before oligomycin injection) − (minimum rate measurement after rotenone/antimycin-A injection); OCR (maximal) = (maximum rate measurement after FCCP injection) − (minimum rate measurement after rotenone/antimycin A injection); OCR (non-mitochondrial respiration) = (minimum rate measurement after rotenone/antimycin A injection); proton leak = (minimum rate measurement after oligomycin injection) – (non-mitochondrial respiration). For the ECAR assay, injection port A on the sensor cartridge was loaded with 10 mM glucose. During the sensor calibration, cells were incubated in a 37 °C non-CO_2 incubator in 180 μL of assay medium (XF base medium with 2 mM L-glutamine, pH 7.4). The plate was immediately placed into the calibrated XFp Extracellular Flux Analyzer™ for the Glycolysis Stress test (Supplementary Fig. 3b). Oligomycin (1 μM) and 50 mM 2-deoxy-D-glucose were loaded for the measurement. ECAR was normalized for the total protein/well and calculated as follows: ECAR (glycolysis) = (maximum rate measurement after glucose injection) − (last rate measurement before glucose injection).

Respiratory enzyme activity in intact and permeabilized cells

The mitochondrial function in intact and permeabilized cells was measured using XFp Extracellular Flux Analyzer™ (Seahorse Bioscience). Assays in intact cells were performed as described previously [46]. Measurement of the activity of mitochondrial respiratory complexes in permeabilized cells was performed according to the manufacturer's instructions. Briefly, intact cells were permeabilized using 1 nmol/L Plasma Membrane Permeabilizer™ (Seahorse Bioscience) immediately before OCR measurement by XFp Extracellular Flux Analyzer™. Oxygen consumption derived from mitochondrial complex I or complex II activity was measured by providing different substrates to mitochondria, such as pyruvate/malate for complex I and succinate for complex II. Rotenone, malonate, and antimycin A were used as specific inhibitors of mitochondrial complexes I, II, and III, respectively [46,47].

Statistical analysis

All experiments were repeated at least twice, and each sample was evaluated in triplicate. Representative data, expressed as the means ± SD, are shown. Differences between treatment groups were evaluated by one-way analysis of variance (ANOVA) or two-way ANOVA, followed by Dunnett's multiple comparison test or *t*-test using GraphPad Prism 7. P-values of < 0.05 were considered statistically significant.

Acknowledgments

This work was supported by the Japan Society for the Promotion of Science KAKENHI, Grants #26670693 and #24592336 to K.H., #25462457 to K.N., and #15K15577 to T.A, and by a research grant from Katano Kai to K.H. and A.O. This works was supported by the research grant B from Kansai Medical University to A.O , the research grant from Kansai Medical University (KMU) research consortium to K.H. and the research grant from Katano Kai to A.O. and K.H.

We would like to thank Editage (www.editage.jp) for English language editing.

Author contributions statement

C.S. performed the experiments, analyzed the data, and co-wrote the manuscript. A.O. and H.T. performed the experiments, contributed to the data analysis and discussion. K.N., M.K, T.S., T.U., Y.M., and T.A.contributed to the data analysis and discussion. J.H. and K.T. provided experimental materials and contributed to discussion. K.H. designed and supervised the study, analyzed the data, and co-wrote the manuscript.

Additional information

Competing financial interests

The authors declare no competing financial interests.

References

1 Kam, P. C. & Cardone, D. Propofol infusion syndrome. *Anaesthesia* **62**, 690-701, doi:10.1111/j.1365-2044.2007.05055.x (2007).

2 Bray, R. J. Propofol infusion syndrome in children. *Paediatr Anaesth* **8**, 491-499 (1998).

3 Parke, T. J. *et al.* Metabolic acidosis and fatal myocardial failure after propofol infusion in children: five case reports. *BMJ* **305**, 613-616 (1992).

4 Finsterer, J. & Frank, M. Propofol Is Mitochondrion-Toxic and May Unmask a Mitochondrial Disorder. *J Child Neurol* **31**, 1489-1494, doi:10.1177/0883073816661458 (2016).

5 Niezgoda, J. & Morgan, P. G. Anesthetic considerations in patients with mitochondrial defects. *Paediatr Anaesth* **23**, 785-793, doi:10.1111/pan.12158 (2013).

6 Fudickar, A. & Bein, B. Propofol infusion syndrome: update of clinical manifestation and pathophysiology. *Minerva Anestesiol* **75**, 339-344 (2009).

7 Bains, R., Moe, M. C., Vinje, M. L. & Berg-Johnsen, J. Sevoflurane and propofol depolarize mitochondria in rat and human cerebrocortical synaptosomes by different mechanisms. *Acta Anaesthesiol Scand* **53**, 1354-1360, doi:10.1111/j.1399-6576.2009.02047.x (2009).

8 Branca, D., Roberti, M. S., Vincenti, E. & Scutari, G. Uncoupling effect of the general anesthetic 2,6-diisopropylphenol in isolated rat liver mitochondria. *Arch Biochem Biophys* **290**, 517-521 (1991).

9 Rigoulet, M., Devin, A., Averet, N., Vandais, B. & Guerin, B. Mechanisms of inhibition and uncoupling of respiration in isolated rat liver mitochondria by the general anesthetic 2,6-diisopropylphenol. *Eur J Biochem* **241**, 280-285 (1996).

10 Cray, S. H., Robinson, B. H. & Cox, P. N. Lactic acidemia and bradyarrhythmia in a child sedated with propofol. *Crit Care Med* **26**, 2087-2092 (1998).

11 Prabhakar, N. R. & Semenza, G. L. Adaptive and maladaptive cardiorespiratory responses to continuous and intermittent hypoxia mediated by hypoxia-inducible factors 1 and 2. *Physiol Rev* **92**, 967-1003, doi:10.1152/physrev.00030.2011 (2012).

12 Murphy, M. P. How mitochondria produce reactive oxygen species. *Biochem J* **417**, 1-13, doi:10.1042/BJ20081386 (2009).

13 Chen, Q., Vazquez, E. J., Moghaddas, S., Hoppel, C. L. & Lesnefsky, E. J. Production of reactive oxygen species by mitochondria: central role of complex III. *J Biol Chem* **278**, 36027-36031, doi:10.1074/jbc.M304854200 (2003).

14 Chandel, N. S. & Schumacker, P. T. Cells depleted of mitochondrial DNA (rho0) yield insight into physiological mechanisms. *FEBS Lett* **454**, 173-176 (1999).

15 Ishikawa, K. *et al.* ROS-generating mitochondrial DNA mutations can regulate tumor cell metastasis. *Science* **320**, 661-664, doi:10.1126/science.1156906 (2008).

16 Ferrannini, E. The target of metformin in type 2 diabetes. *N Engl J Med* **371**, 1547-1548, doi:10.1056/NEJMcibr1409796 (2014).

17 Wheaton, W. W. *et al.* Metformin inhibits mitochondrial complex I of cancer cells to reduce tumorigenesis. *Elife* **3**, e02242, doi:10.7554/eLife.02242 (2014).

18 Gui, D. Y. *et al.* Environment Dictates Dependence on Mitochondrial Complex I for NAD+ and Aspartate Production and Determines Cancer Cell Sensitivity to Metformin. *Cell Metab* **24**, 716-727, doi:10.1016/j.cmet.2016.09.006 (2016).

19 Bridges, H. R., Jones, A. J., Pollak, M. N. & Hirst, J. Effects of metformin and other biguanides on oxidative phosphorylation in mitochondria. *Biochem J* **462**, 475-487, doi:10.1042/BJ20140620 (2014).

20 Matsuzaki, S. & Humphries, K. M. Selective inhibition of deactivated mitochondrial complex I by biguanides. *Biochemistry* **54**, 2011-2021, doi:10.1021/bi501473h (2015).

21 Luengo, A., Sullivan, L. B. & Heiden, M. G. Understanding the complex-I-ty of metformin action: limiting mitochondrial respiration to improve cancer therapy. *BMC*

Biol **12**, 82, doi:10.1186/s12915-014-0082-4 (2014).

22 Ludbrook, G. L., Visco, E. & Lam, A. M. Propofol: relation between brain concentrations, electroencephalogram, middle cerebral artery blood flow velocity, and cerebral oxygen extraction during induction of anesthesia. *Anesthesiology* **97**, 1363-1370 (2002).

23 Vanlander, A. V. *et al.* Possible pathogenic mechanism of propofol infusion syndrome involves coenzyme q. *Anesthesiology* **122**, 343-352, doi:10.1097/ALN.0000000000000484 (2015).

24 Krajcova, A., Waldauf, P., Andel, M. & Duska, F. Propofol infusion syndrome: a structured review of experimental studies and 153 published case reports. *Crit Care* **19**, 398, doi:10.1186/s13054-015-1112-5 (2015).

25 Yang, N., Liang, Y., Yang, P., Yang, T. & Jiang, L. Propofol inhibits lung cancer cell viability and induces cell apoptosis by upregulating microRNA-486 expression. *Braz J Med Biol Res* **50**, e5794, doi:10.1590/1414-431X20165794 (2017).

26 Konno, A. *et al.* Continuous monitoring of caspase-3 activation induced by propofol in developing mouse brain. *Int J Dev Neurosci* **51**, 42-49, doi:10.1016/j.ijdevneu.2016.04.007 (2016).

27 Meng, C. *et al.* Propofol induces proliferation partially via downregulation of p53 protein and promotes migration via activation of the Nrf2 pathway in human breast cancer cell line MDA-MB-231. *Oncol Rep* **37**, 841-848, doi:10.3892/or.2016.5332 (2017).

28 Cui, W. Y., Liu, Y., Zhu, Y. Q., Song, T. & Wang, Q. S. Propofol induces endoplasmic reticulum (ER) stress and apoptosis in lung cancer cell H460. *Tumour Biol* **35**, 5213-5217, doi:10.1007/s13277-014-1677-7 (2014).

29 Kroemer, G., Dallaporta, B. & Resche-Rigon, M. The mitochondrial death/life regulator in apoptosis and necrosis. *Annu Rev Physiol* **60**, 619-642,

doi:10.1146/annurev.physiol.60.1.619 (1998).

30 Roberts, R. J. *et al.* Incidence of propofol-related infusion syndrome in critically ill adults: a prospective, multicenter study. *Crit Care* **13**, R169, doi:10.1186/cc8145 (2009).

31 Cohen, P. J. Effect of anesthetics on mitochondrial function. *Anesthesiology* **39**, 153-164 (1973).

32 Ishikawa, K. *et al.* Enhanced glycolysis induced by mtDNA mutations does not regulate metastasis. *FEBS Lett* **582**, 3525-3530, doi:10.1016/j.febslet.2008.09.024 (2008).

33 Ishikawa, K. & Hayashi, J. A novel function of mtDNA: its involvement in metastasis. *Ann N Y Acad Sci* **1201**, 40-43, doi:10.1111/j.1749-6632.2010.05616.x (2010).

34 Miyamoto, Y., Miyashita, T., Takaki, S. & Goto, T. Perioperative considerations in adult mitochondrial disease: A case series and a review of 111 cases. *Mitochondrion* **26**, 26-32, doi:10.1016/j.mito.2015.11.004 (2016).

35 Savard, M. *et al.* Propofol-related infusion syndrome heralding a mitochondrial disease: case report. *Neurology* **81**, 770-771, doi:10.1212/WNL.0b013e3182a1aa78 (2013).

36 El-Mir, M. Y. *et al.* Dimethylbiguanide inhibits cell respiration via an indirect effect targeted on the respiratory chain complex I. *J Biol Chem* **275**, 223-228 (2000).

37 Owen, M. R., Doran, E. & Halestrap, A. P. Evidence that metformin exerts its anti-diabetic effects through inhibition of complex 1 of the mitochondrial respiratory chain. *Biochem J* **348 Pt 3**, 607-614 (2000).

38 Drahota, Z. *et al.* Biguanides inhibit complex I, II and IV of rat liver mitochondria and modify their functional properties. *Physiol Res* **63**, 1-11 (2014).

39 Finsterer, J. & Scorza, F. A. Effects of antiepileptic drugs on mitochondrial functions, morphology, kinetics, biogenesis, and survival. *Epilepsy Res* **136**, 5-11, doi:10.1016/j.eplepsyres.2017.07.003 (2017).

40 Zhang, C. *et al.* Valproic Acid Promotes Human Glioma U87 Cells Apoptosis and

Inhibits Glycogen Synthase Kinase-3beta Through ERK/Akt Signaling. *Cell Physiol Biochem* **39**, 2173-2185, doi:10.1159/000447912 (2016).

41 Uppala, R. *et al.* Aspirin increases mitochondrial fatty acid oxidation. *Biochem Biophys Res Commun* **482**, 346-351, doi:10.1016/j.bbrc.2016.11.066 (2017).

42 Moreno-Lastres, D. *et al.* Mitochondrial complex I plays an essential role in human respirasome assembly. *Cell Metab* **15**, 324-335, doi:10.1016/j.cmet.2012.01.015 (2012).

43 Okamoto, A. *et al.* HIF-1-mediated suppression of mitochondria electron transport chain function confers resistance to lidocaine-induced cell death. *Sci Rep* **7**, 3816, doi:10.1038/s41598-017-03980-7 (2017).

44 Yokota, M. *et al.* Generation of trans-mitochondrial mito-mice by the introduction of a pathogenic G13997A mtDNA from highly metastatic lung carcinoma cells. *FEBS Lett* **584**, 3943-3948, doi:10.1016/j.febslet.2010.07.048 (2010).

45 Okamoto, A. *et al.* The antioxidant N-acetyl cysteine suppresses lidocaine-induced intracellular reactive oxygen species production and cell death in neuronal SH-SY5Y cells. *BMC Anesthesiol* **16**, 104, doi:10.1186/s12871-016-0273-3 (2016).

46 Salabei, J. K., Gibb, A. A. & Hill, B. G. Comprehensive measurement of respiratory activity in permeabilized cells using extracellular flux analysis. *Nat Protoc* **9**, 421-438, doi:10.1038/nprot.2014.018 (2014).

47 Cheng, G. *et al.* Mitochondria-Targeted Analogues of Metformin Exhibit Enhanced Antiproliferative and Radiosensitizing Effects in Pancreatic Cancer Cells. *Cancer Res* **76**, 3904-3915, doi:10.1158/0008-5472.CAN-15-2534 (2016).

Tables

Table 1 Identification of pathogenic mutations in mtDNA sequences

Position	Gene	Amino acid change	Mouse strain	Cell lines			
			C57BL/6	P29	A11	B82	B82M
T6589C	*COI*	V421A	T	T	T	C	C
G9348A	*COIII*	V281I	G	G	G	A	A
13885insC	*ND6*	Flame-shift	-	-	-	-	C
G13997A	*ND6*	P25L	G	G	A	G	G

Table 2 Genetic characteristics of parent cells and their transmitochondrial cybrids

Cell lines	Nuclear genotypes	Fusion combinations		
		Nuclear donors	X	mtDNA donors
ρ0P29	P29	ρ0P29		(-)
P29mtA11	P29	ρ0P29	X	enA11
P29mtB82M	P29	ρ0P29	X	enB82M
P29mtCOIM	P29	ρ0P29	X	enB82
P29mtΔ	P29	ρ0P29	X	enB82mtΔ

Figure Legends

Figure 1 Propofol induced caspase activation and cell death in a concentration- and time-dependent manner

SH-SY5Y cells were exposed to the indicated concentrations (12.5, 25, 50, 100, and 150 μM) of propofol for 3, 6, and 12 h (b and f) and 6 h (a–c) Caspase-3/7 (n = 5) (a and b) and caspase-9 (n = 5) (c) activities in each treatment group at different time points. (d) Percentages of cell death in treated and untreated cell populations. Cell death was evaluated by measuring the levels of LDH in culture supernatants (n = 3). Treatment with lysis buffer served as a control. (e and f) Cells were harvested, and percentages of cell death were measured by flow cytometry. The ratio of PI-positive and/or annexin V-positive cells [(Q1 + Q2 + Q4)/(Q1 + Q2 + Q3 + Q4)] was used to calculate the percentage of dead cells (Supplemental Fig. 1a) (n = 3). (g) Average mitochondrial membrane potential ($\Delta\Psi m$) of untreated cells and cells treated with indicated concentrations (25, 50, and 100 μM) of propofol (n = 3) for 6 h. Values indicate the ratio [Q2/(Q2 + Q4)] of green JC-1 monomers (527 nm emission) to red aggregates (590 nm emission). Data presented in (a–g) are expressed as the mean ± SD. Differences between treatment groups were evaluated by one-way ANOVA, followed by Dunnett's multiple comparison test (a, c, d, e, and g), or by two-way ANOVA, followed by Dunnett's multiple comparison test (b and f). *$p < 0.05$ compared to the control cell population (incubation for 0 h, no treatment).

Figure 2 Oxygen metabolism and ROS generation in SH-SY5Y cells treated with propofol

OCR (a, b, and e) and ECAR (c, d and f) in SH-SY5Y cells exposed to the indicated concentrations of propofol (12.5, 25, 50, and 100 μM) for 6 h (b and d) or 0, 3, 6, and 12 h (e and f). Data presented in (b, d–f) are expressed as the means ± SD. Differences between treatment groups were evaluated by one-way ANOVA, followed by Dunnett's multiple comparison test (b and d), or by two-way ANOVA, followed by Dunnett's multiple comparison

test (e and f). (g) ROS production in SH-SY5Y cells exposed to 25, 50, and 100 μM propofol (n = 3) for 3 h. MFI: median fluorecent intensity *p < 0.05 compared to the control cell population.

Figure 3 Involvement of functional mitochondria in propofol-induced caspase activation and cell death

P29 cells and cells of the ρ0P29 derivative lacking mtDNA were exposed to the indicated concentrations (25, 50, and 100 μM) of propofol for 6 h. (a) Caspase-3/7 activity in each treatment group (n = 3) at 6 h. (b) Cells were harvested, and percentages of cell death were measured by flow cytometry. The ratio of PI-positive and/or annexin V-positive cells [(Q1 + Q2 + Q4)/(Q1 + Q2 + Q3 + Q4)] was used to calculate the percentage of dead cells (Supplemental Fig. 1a) (n = 3). Differences between treatment groups were evaluated by one-way ANOVA, followed by Dunnett's multiple comparison test. *p < 0.05 compared to the control cell population; #p < 0.05 compared to the indicated experimental groups.

Figure 4 Effects of propofol on each complex of the mitochondrial electron transport chain

Mitochondrial ETC-mediated respiratory activities of complexes I (a), II (b), III (c), and IV (d) were assayed by a flux analyzer-based protocol. SH-SY5Y cells were exposed to 100 and 200 μM propofol for 6 h and subjected to the assay. Differences between treatment groups were evaluated by one-way ANOVA, followed by Dunnett's multiple comparison test. *p < 0.05 compared to the control cell population.

Figure 5 Synergistic effects of propofol and mitochondrial ETC inhibitors on caspase activity and cell death

Levels of caspase-3/7 activity and cell death of SH-SY5Y cells treated with propofol and mitochondrial ETC inhibitors. Cells were treated with 12.5, 25 or 50 μM propofol and either 100 nM rotenone, 4 μM oligomycin, or 25 μg/mL antimycin A and subjected to (a) a caspase-3/7 activity assay (n = 3) and (b) cell death assay. Percentages of cell death were measured by flow cytometry. The ratio of PI-positive and/or annexin V-positive cells [(Q1 + Q2 + Q4)/(Q1 + Q2 + Q3 + Q4)] was used to calculate the percentage of dead cells (Supplemental Fig. 1a) (n = 3). All data are expressed as the means ± SD. *$p < 0.05$ compared with control cells (no treatment); #$p < 0.05$ compared with the indicated groups. rot: rotenone; olig: oligomycin; anti: antimycin A.

Figure 6 Effects of propofol on caspase activity and cell death in various transmitochondrial cybrid cells

(a) OCR and (b) ECAR of P29, its cybrid cells, and ρ0 cells. (c and d) P29, its cybrid cells, and ρ0 cells were exposed to the indicated concentrations (12.5, 25, and 50 μM) of propofol for 6 h. Caspase-3/7 activity in each treatment group (n = 3) at 6 h (c). Cells were harvested, and percentages of cell death were measured by flow cytometry. The ratio of PI-positive and/or annexin V-positive cells [(Q1 + Q2 + Q4)/(Q1 + Q2 + Q3 + Q4)] was used to calculate the percentage of dead cells (n = 3) (d). Data presented in (a–d) are expressed as the means ± SD. Differences between treatment groups were evaluated by one-way ANOVA, followed by Dunnett's multiple comparison test (a and b), or by two-way ANOVA, followed by Dunnett's multiple comparison test (c and d). *$p < 0.05$ compared to the control cell population. A11: P29mtA11 cells, B82M: P29mtB82M cells, COIM: P29mtCOIM cells, mtΔ: P29mtΔ cells.

Figure 7 Synergistic effects of propofol and metformin on caspase activity and cell death

(a) OCR and (b) ECAR of SH-SY5Y cells exposed to the indicated concentrations of metformin (2.5, 5, 10, and 20 mM) for 6 h. (c) SH-SY5Y cells were exposed to 25 μM propofol with or

without 5 mM metformin, and ROS production was determined (n = 3). (d and e) SH-SY5Y cells were exposed to the indicated concentrations (12.5, 25, 50, and 100 μM) of propofol with or without 5 mM metformin for 6 h. (d) Caspase-3/7 activity in each treatment group (n = 3). (e) Cells were harvested, and percentages of cell death were measured by flow cytometry. The ratio of PI-positive and/or annexin V-positive cells [(Q1 + Q2 + Q4)/(Q1 + Q2 + Q3 + Q4)] was used to calculate the percentage of dead cells (n = 3). Data presented in (a–e) are expressed as the means ± SD. Differences between treatment groups were evaluated by one-way ANOVA, followed by Dunnett's multiple comparison test (a, b, and c), or by two-way ANOVA, followed by Dunnett's multiple comparison test (d and e). *$p < 0.05$ compared to the control cell population; #$p < 0.05$ compared to the indicated experimental groups.

Figure 8 The schematic representation of the findings of this study

Clinically relevant concentrations of propofol used within a clinically relevant exposure time suppressed the mitochondrial function. Propofol induces generation of reactive oxygen species (ROS) and the metabolic reprogramming by targeting complexes I and III of mitochondria electron transport chain (ETC). The predisposition to mitochondrial dysfunction, caused by genetic mutations and pharmacological suppression of ETC by biguanides facilitates the cell death and caspase activation induced by propofol. The process may constitute the molecular basis of propofol infusion syndrome (PRIS). OCR: oxygen consumption rate, ECAR: extracellular acidification rate

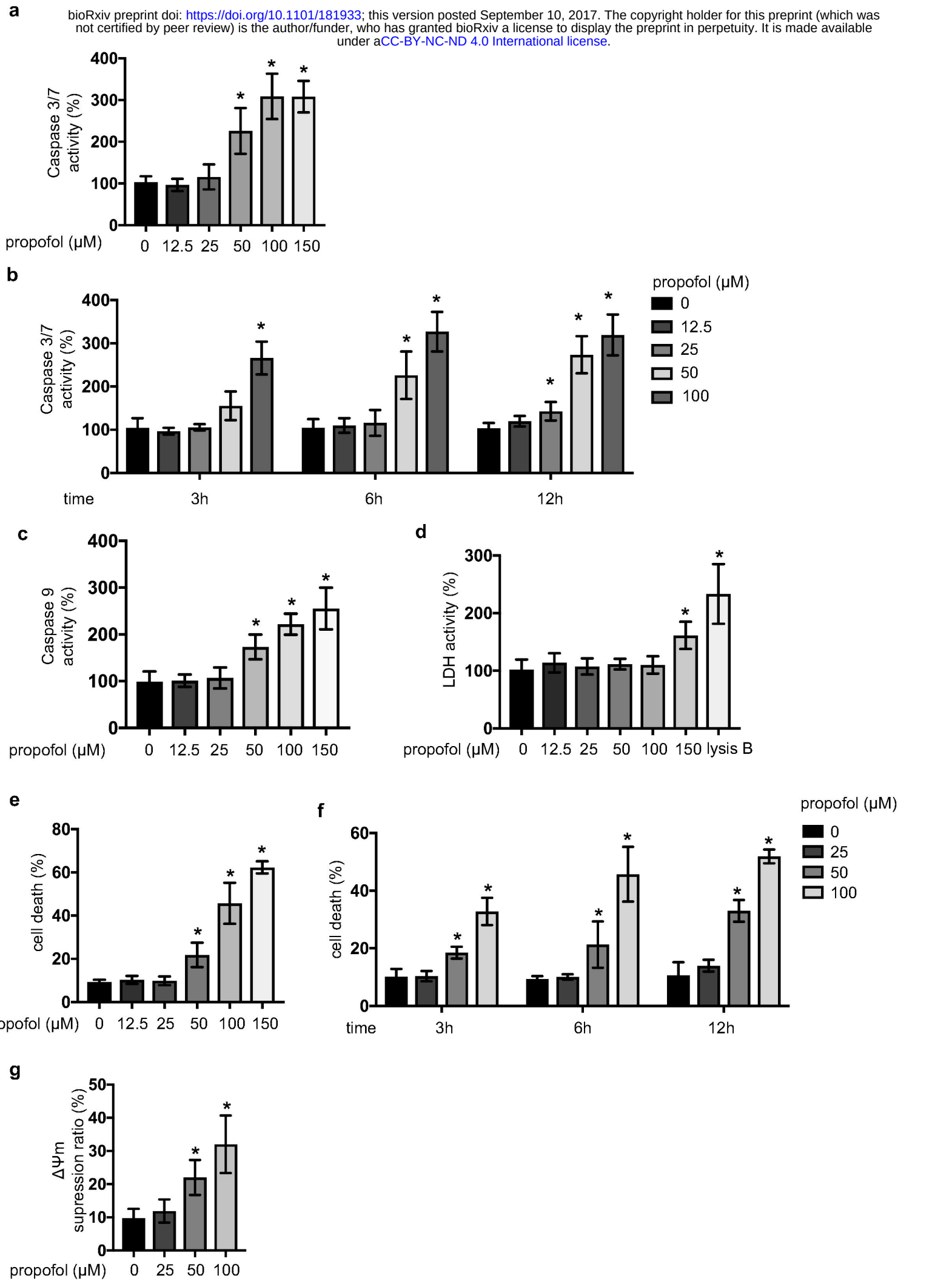

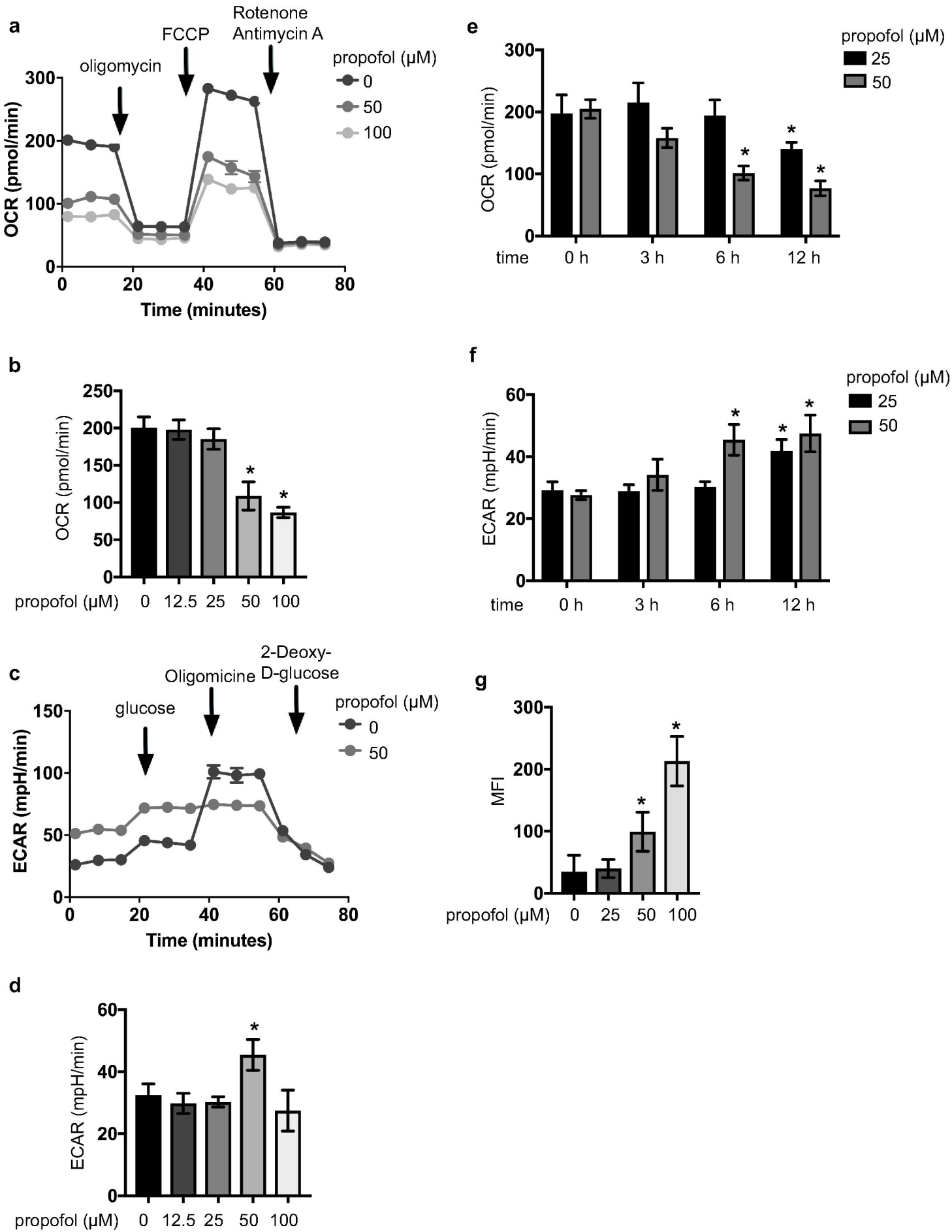

a

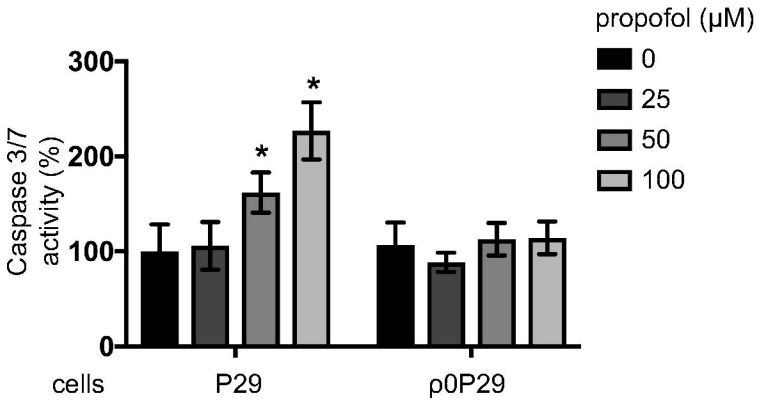

b